Clinical Oral Investigations (2023) 27:1277–1288
https://doi.org/10.1007/s00784-022-04761-x

RESEARCH

Diagnostic accuracy of fused CBCT images in the evaluation of temporomandibular joint condylar bone resorption

Ji-ling Feng[1] · Ruo-han Ma[1] · Han Du[1,2,3] · Yan-ping Zhao[1,4] · Juan-hong Meng[4] · Gang Li[1]

Received: 28 June 2022 / Accepted: 18 October 2022 / Published online: 27 October 2022

Abstract

Objectives To evaluate the diagnostic accuracy of fused CBCT images for patients with condylar bone resorption of temporomandibular joint (TMJ) osteoarthrosis.

Materials and methods Forty-two TMJs from twenty-one patients were included. Bone resorption of condyles evaluated by three experts was used as the reference standard. Three oral and maxillofacial radiology residents evaluated the resorption of condyles with a five-point scale for the four sets of images (two consecutive CBCT images without fusion, fused 2D cross-sectional images, fused 3D images, and combining fused 2D cross-sectional images and fused 3D images) randomly and independently. Each set of images was evaluated at least 1 week apart, and a second evaluation was performed 4 weeks later. Intraclass correlation coefficients were calculated to assess the intra- and inter-observer agreement. The areas under the ROC curves (AUCs) were compared among the four image sets using the *Z* test.

Results Twenty-four TMJs were determined as condylar bone resorption, and eighteen were determined as no obvious change. The average AUC values from the three observers for the three fused image sets (0.94, 0.93, 0.93) were significantly higher than the image set without fusion ($p < 0.01$). The intra- and inter-observer agreement on the three fused image sets (0.70–0.89, 0.91–0.92) was higher than the image set without fusion (0.37–0.63, 0.75).

Conclusions Fused CBCT images of TMJ osteoarthrosis patients can intuitively display the condylar bone resorption and significantly improve the diagnostic accuracy.

Clinical relevance Fused CBCT images can help clinicians intuitively observe bone changes of the condyle in TMJ osteoarthrosis patients.

Keywords Temporomandibular joint · Diagnosis · Cone-beam computed tomography · Registration

Introduction

The temporomandibular joint (TMJ) is involved in many functional activities of the craniomaxillofacial system such as chewing, swallowing, and speaking. Excessive overloading surpassing the physiological capacity of TMJ may lead to inflammation and accompanied arthralgia and then induce TMJ osteoarthrosis, a kind of TMJ degenerative change [1–4]. For diagnosing TMJ osteoarthrosis, medical imaging examination constitutes an indispensable element in nowadays clinical work. As a kind of three-dimensional medical imaging examination technique, cone-beam computed tomography (CBCT) with a higher spatial resolution and lower radiation dose compared to helical CT is more effective in detecting TMJ condylar bone changes, such as erosions, osteophytes, flattening, sclerosis, and abnormal condylar shapes [5–10].

TMJ osteoarthrosis is a chronic disease with long-term therapy. Clinically, radiologists or clinicians will compare CBCT images taken at different times to observe the condylar bone changes during follow-up. The research on comparing condylar bone change mainly includes the direct observation method [11], superimposition [12, 13], surface reconstruction, and color map [14–16]. Koyama J. et al. reported the direct observation method for condylar bone changes with helical computed tomography images [11]. However, this method cannot provide sufficient information when the bone change is small and the condylar edge is irregular and fuzzy, or the condylar

✉ Gang Li
kqgang@bjmu.edu.cn

Extended author information available on the last page of the article

position is changed. This problem may be solved by the superimposition of two CBCT images taken at different time points. Park SB et al. and Soo-Min Ok et al. used superimposition to align the viewing angles of two CBCT images and studied the condylar head remodeling by metric analysis or direct observation [12, 13]. This is not intuitive and time-consuming, especially when the change is very small. For intuitively displaying and assessing condylar bone changes, some researchers used the color-coded map of the reconstructed condylar surface that was obtained from the segmentation and superimposition of two time point CBCT images for qualitative and quantitative evaluation [14–16]. However, this method is still time-consuming and may lead to error, especially when the condylar morphology changes greatly since the Euclidean distance of the color-coded map is calculated from the distance between the two nearest points, not the two corresponding points. To solve the problems, we have proposed an image registration and fusing method for the intuitive observation and evaluation of condylar bone changes [17]. By this method, the fused 2D cross-sectional images and the fused 3D images from different time points of CBCT images could be created.

Thus, the main purpose of the present study was to evaluate the consistency and reliability of the method in the evaluation of condylar bone resorption. To achieve this purpose, we first compared the direct observation method to the fusion method for the detection of condylar bone changes and then investigated whether the combined observation of fused 2D cross-sectional images and 3D images would further improve its diagnostic accuracy.

The hypothesis of the present study was that the fused 2D cross-sectional images and the fused 3D images are superior to the direct observation method for the determination of bone resorption during follow-up.

Materials and methods

Subjects

According to a longitudinal study, the prevalence of condylar bone resorption in TMJ osteoarthrosis patients during the follow-up was 62.7% [18]. Assuming that both sensitivity and specificity for the detection of condylar bone resorption were 0.9, 25 positive cases with bone resorption and 15 negative cases without bone resorption were required, and this resulted in a total of 40 cases.

The WHO international clinical trial registration (ChiCTR2200060049) was completed for this study. This study was approved by the institutional review board (PKUSSIRB-201944056), and the exemption of informed consent had been granted because this was a retrospective study. This study included 42 TMJs from 21 patients who visited the Center for Temporomandibular Disorders and Orofacial Pain in Peking University School and Hospital of Stomatology from 2014 to 2020. The inclusion criteria were as follows: (1) by overviewing clinical symptoms, medical history, and imaging examination, the patient was diagnosed with TMJ osteoarthrosis according to Diagnostic Criteria for Temporomandibular Disorders (DC/TMD) [19]; (2) the acquired image data included the full TMJ structures and no motion artifact; (3) the interval between the two CBCT examinations was not less than 3 months; (4) the age of the patient was beyond 18 years old. The exclusion criteria were as follows: (1) the patient had no definite diagnosis of TMJ osteoarthrosis; (2) movement or metal artifacts affected the observation of condylar bone; (3) the age of the patient was under 18 years old.

CBCT image acquisition

Each CBCT scan was acquired in 360° rotation for the patient whose Frankfort plane was parallel to the floor in a sitting position. The thyroid collar was used. Images of each TMJ were obtained in the maximal intercuspation. Scans were performed using CBCT unit 3D Accuitomo 170 (J Morita Mfg., Corp., Kyoto, Japan). The exposure parameters were as follows: scanning time of 17.5 s, tube current of 4–5 mA, tube potential of 80–90 kVp, and field of view (FOV) was 6cm × 6cm. The scan included one side of TMJs and part of the mandible.

All the image datasets obtained from CBCT were reconstructed with a voxel size of 0.125 mm and exported as Digital Imaging and Communications in Medicine (DICOM) format.

Image segmentation

The segmentation of two consecutive CBCT datasets was conducted by the Amira visual software (version 2020.2, Thermo Fisher Scientific, France). After we input the consecutive CBCT datasets of the same patient, the threshold of the 2D cross-sectional images and the 3D images were individually adjusted in the multiplanar viewer module. However, for each patient, the range of threshold was constant. The lower threshold was between 200 and 300, and the upper limit was 1400–1500 for all the patients.

Image registration and fusion

The registration and fusion of two consecutive CBCT datasets were carried out by the Amira visual software,

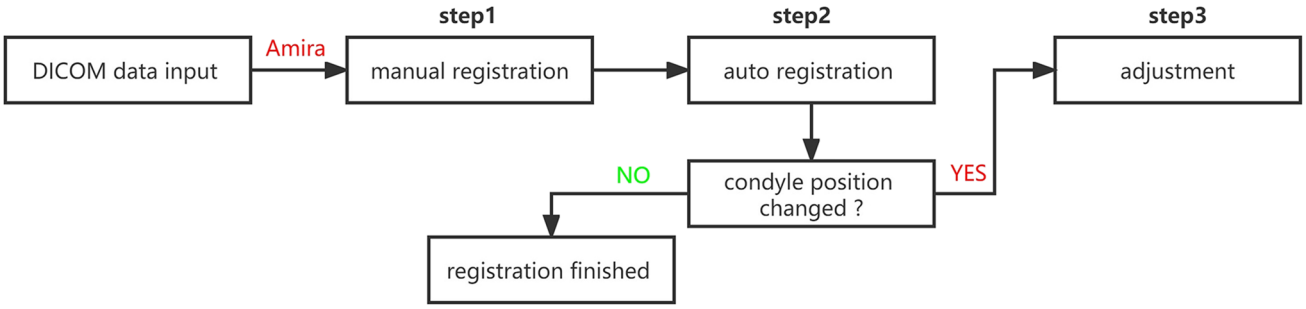

Fig. 1 Flow chart of the registration process

and the registration process was conducted in the multiplanar viewer module. The process of registration included three steps, namely, manual registration, auto registration, and manual adjustment (Fig. 1). Because the image datasets used for registration were from the same patient taken at different time points, the rigid transform model was adopted. More detailed information could be found in the previous study [17]. To observe the condylar bone changes, the voxel registration was performed based on the mandibular ramus and the coronoid process, which were relatively stable for patients with TMJ osteoarthrosis. However, the cranial base took the greater part of CBCT image sets; the outcome of auto registration usually was done by aligning the cranial base. In this case, only if the condyle position relative to the cranial base was not changed, the condyle will be aligned. Otherwise, the manual adjustment was an important step to assure that the condyles were aligning up. The first CBCT dataset was set as the preliminary data which appeared in grayscale, while the second CBCT dataset was set as the overlapped data which appeared in luminous yellow color for the fused 2D cross-sectional image sets. For the fused volume rendering 3D fused image sets, the two consecutive image sets appeared in red and green, respectively.

To evaluate the registration accuracy, two radiologists with at least 3 years of experience in CBCT image interpretation evaluated the registered images using the subjective evaluation method of a 5-point (1-very poor, 2-poor, 3-average, 4-good, 5-very good) system. Very poor means the images after registration were very serious hindrance to viewing; poor means the images after registration hinder viewing; average means it can be seen that the quality of the images after registration changes which slightly hinders viewing; good means the quality change can be seen, but it does not hinder viewing; very good means there is no change in image quality. Only those registered images that were scored as 4 or 5 were kept for further observation and analysis. Otherwise, the registration was adjusted until the score was greater than or equal to point 4. This was to ensure that the quality of registration was acceptable.

For the evaluation of registration repeatability, 84 datasets from 42 TMJs repeatedly registered one more time after 2 weeks. The change of coordinate values, which included the displacement translation values of the *X*, *Y*, *Z* axis and the position and rotation angle of the *X*, *Y*, *Z* rotation axis of 42 overlay datasets, were recorded.

Image evaluation

One specialist with an experience of over 25 years in oral and maxillofacial radiology and two certified specialists with an experience of over 30 years in oral and maxillofacial surgery (mainly for the diagnosis and conservative treatment of TMJ disease) acted as an expert panel. The specialists independently determined whether any condyle resorption has occurred based on the two consecutive CBCT sets without fusion, fused 2D cross-sectional images, and fused 3D images, respectively. In case the determination was not the same, a consensus was reached in the end.

Three oral and maxillofacial radiology residents with at least 3 years of experience in CBCT image interpretation acted as observers. Before evaluation, the observers were calibrated with an additional session of images in which the definition of condyle bone changes, the theory of the image registration technique, and the strategy of adjusting display parameters of fused images were explained and demonstrated. The example images without condyle resorption are presented in Fig. 2, and the example images with tiny bone resorption and obvious bone resorption are shown in Figs. 3 and 4, respectively.

Three residents evaluated the condyle bone change in the 42 pairs of TMJs in four sets of images randomly and independently: (1) CBCT images at two time points without fusion (Figs. 2, 3, and 4a–f); (2) fused 2D cross-sectional CBCT images (Figs. 2, 3, and 4g–i); (3) fused 3D images (Figs. 2, 3, and 4j–l); (4) combination of

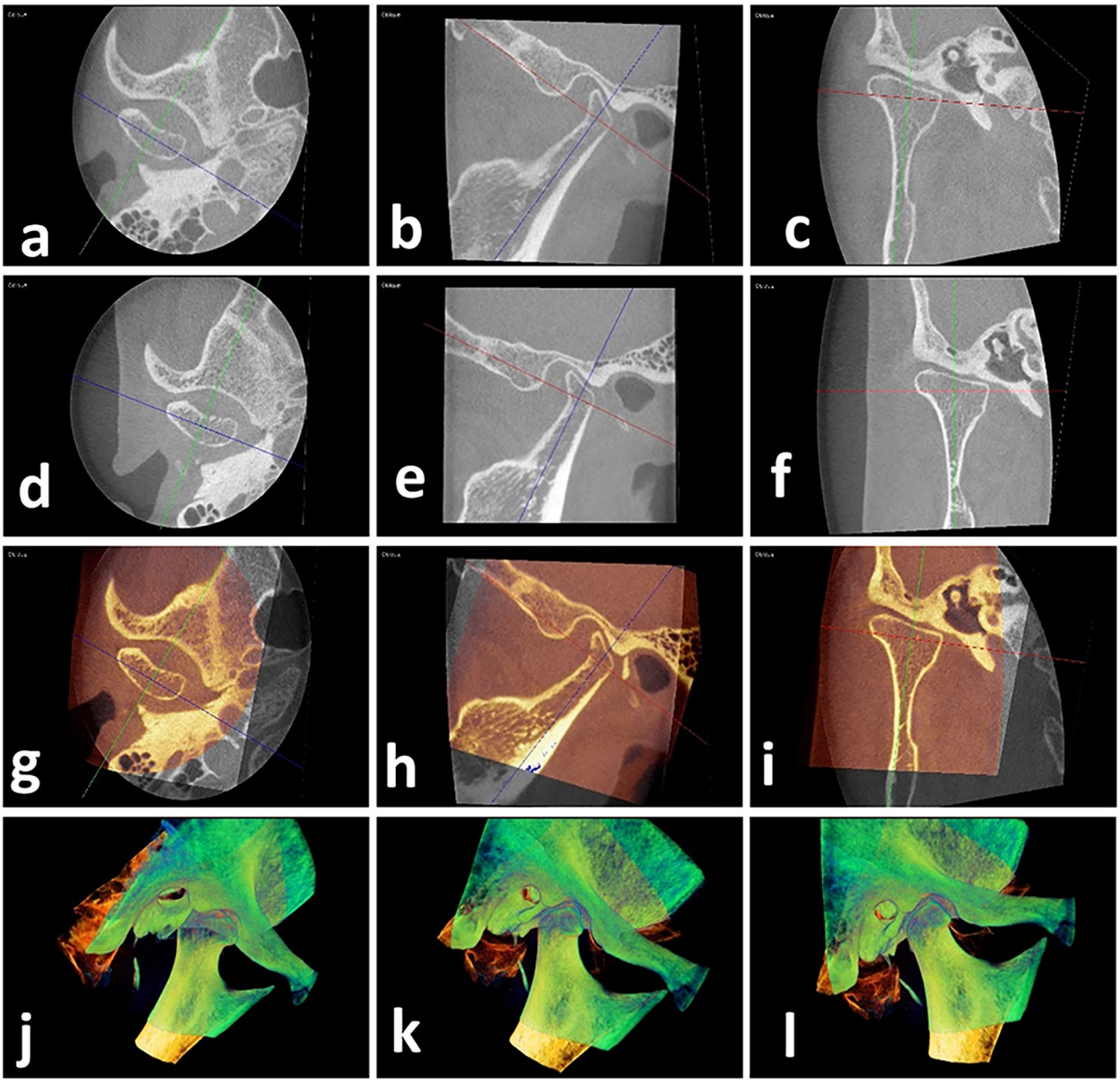

Fig. 2 Example images for the condyle without bone resorption. Axial (**a**), oblique coronal (**b**), and oblique sagittal (**c**) view of the T1 CBCT images; axial (**d**), oblique coronal (**e**), and oblique sagittal (**f**) view of the T2 CBCT images; axial (**g**), oblique coronal (**h**), and oblique sagittal (**i**) view of the fused sectional CBCT images. **j–l** Fused 3D images in different view angles. T1, the previous time CBCT scanning; T2, the later time CBCT scanning; CBCT, cone-beam CT; 3D, three-dimensional

images in group (2) and group (3). Each set of images was observed at least 1 week apart. There were five choices offered to the observers for evaluating the condylar bone changes: 1, definitely resorbed; 2, probably resorbed; 3, questionable; 4, probably not resorbed; and 5, definitely not resorbed.

All images were randomly displayed on a Nio Color 5.8 MP (MDNC-6121) display (Barco NV, Kortrijk, Belgium) in a quiet and dim room. While evaluating, observers could adjust images' position, angle, brightness, contrast, and threshold freely to assist in observation. There was no time limit for evaluation.

For the evaluation of the intra-observer consistency, a second evaluation was performed under the same conditions after 4 weeks by the same observers. Twenty-two TMJs were randomly selected from the 42 TMJs for the second evaluation.

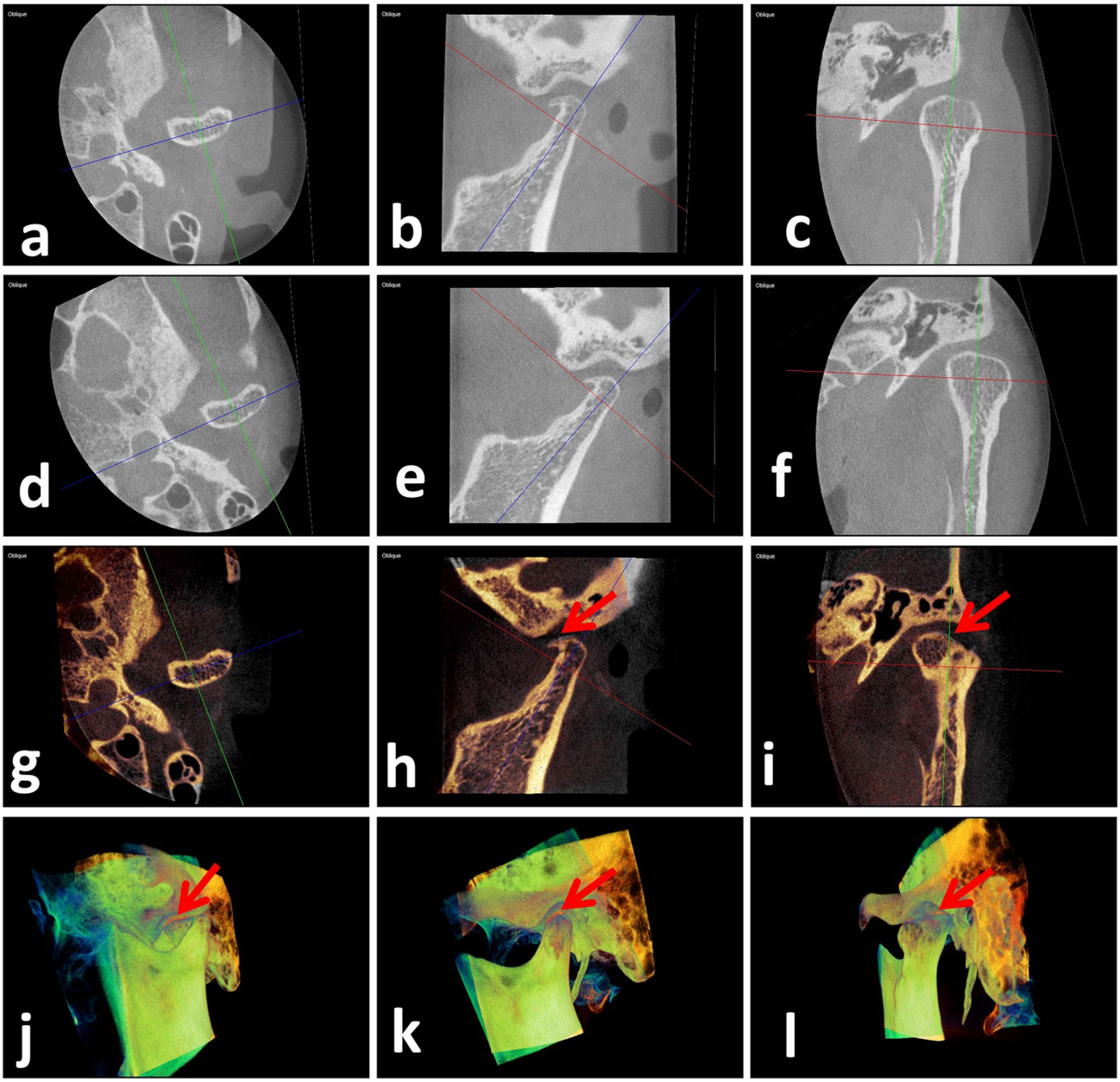

Fig. 3 Example images for the condyle with tiny bone resorption. Axial (**a**), oblique coronal (**b**), and oblique sagittal (**c**) view of the T1 CBCT images; axial (**d**), oblique coronal (**e**), and oblique sagittal (**f**) view of the T2 CBCT images; axial (**g**), oblique coronal (**h**), and oblique sagittal (**i**) view of the fused sectional CBCT images. The gray area pointed by the red arrow indicates tiny bone resorption. **j–l** Fused 3D images in different view angles. The red area pointed by the red arrow indicates tiny bone resorption. T1, the previous time CBCT scanning; T2, the later time CBCT scanning; CBCT, cone-beam CT; 3D, three-dimensional

Statistical analysis

Sample size calculation was made with Power Analysis and Sample Size (PASS) software package V.21.0.3.0 (NCSS, LLC, Kaysville, Utah, USA). Data analysis was conducted using the IBM SPSS Statistics for windows V.25.0 (IBM Crop., Armonk, NY, USA) and MedCalc Statistical Software version 20.027 (MedCalc Software bvba, Ostend, Belgium).

Wilcoxon signed rank test was used to determine the statistical significance of the repeatability of registration. A p-value of 0.05 or less was considered significant.

Intraclass correlation coefficients (ICCs) were calculated to assess the intra- and inter-observer agreement.

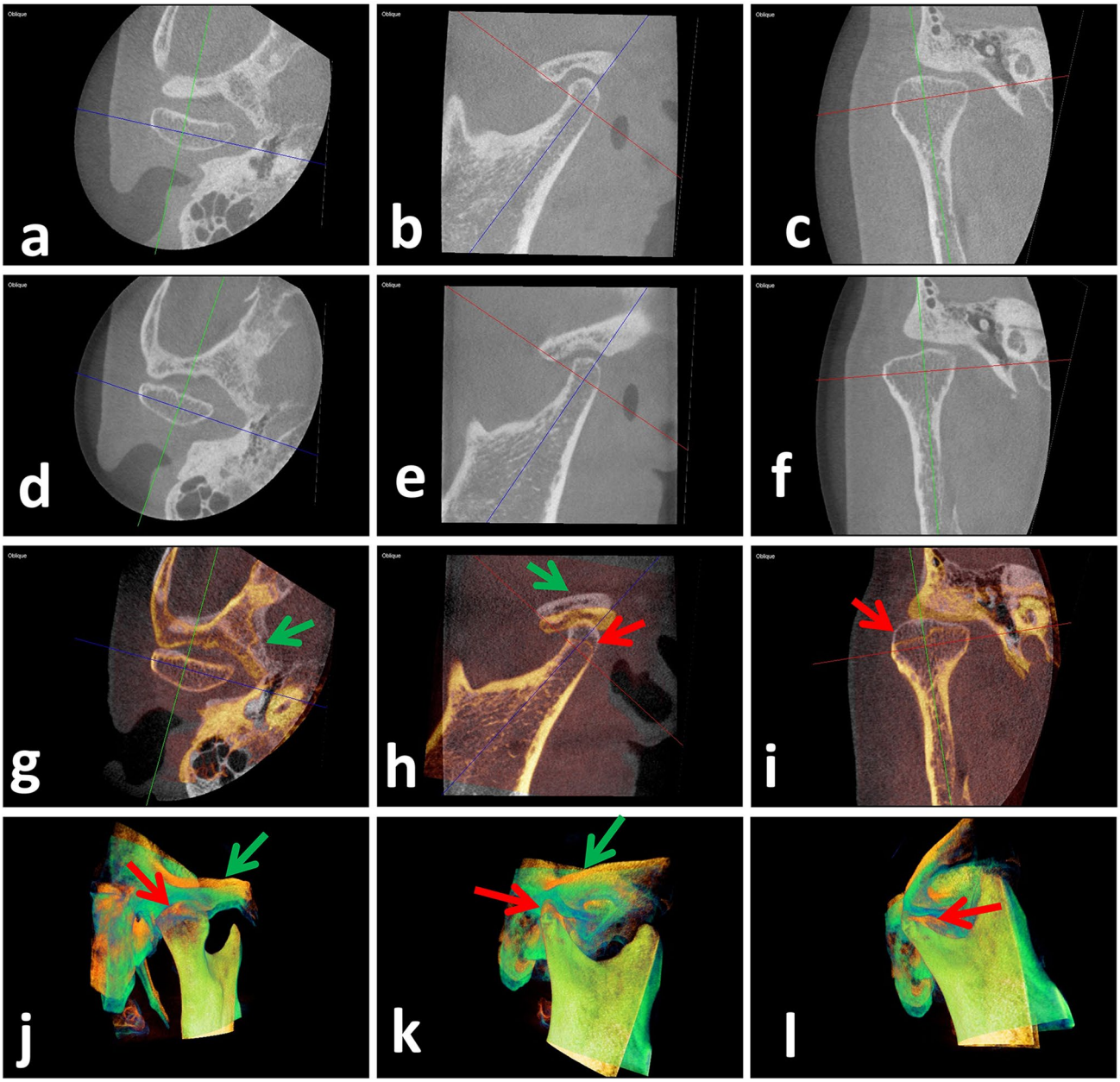

Fig. 4 Example images for the condyle with obvious resorption. Axial (**a**), oblique coronal (**b**), and oblique sagittal (**c**) view of the T1 CBCT images; axial (**d**), oblique coronal (**e**), and oblique sagittal (**f**) view of the T2 CBCT images; axial (**g**), oblique coronal (**h**), and oblique sagittal (**i**) view of the fused sectional CBCT images. The gray area pointed by the red arrow indicates obvious bone resorption, and the gray area pointed by the green arrow indicates the position change of the mandible relative to the cranial base. **j–l** Fused 3D images in different view angles. The red area pointed by the red arrow indicates obvious bone resorption, and the red area pointed by the green arrow indicates the position change of the mandible relative to the cranial base. T1, the previous time CBCT scanning; T2, the later time CBCT scanning; CBCT, cone-beam CT; 3D, three-dimensional

ICC estimates and their 95% confident intervals were calculated based on a single-rating (intra-agreement)/mean-rating(inter-agreement), absolute-agreement, 2-way mixed-effects model. The ICC values were interpreted as poor (< 0.50), moderate (0.50–0.75), good (0.75–0.90), or excellent (> 0.90) in agreement [20].

Scores from each observer generated a pooled ROC curve for four groups of image sets. The areas under the

Table 1 Wilcoxon signed rank test for the repeatability of registration

	TX2 — TX1	TY2 — TY1	TZ2 — TZ1	RX2 — RX1	RY2 — RY1	RZ2 — RZ1	R2 — R1
Z	− .106[a]	− 1.432[a]	− .669[b]	− .031[a]	− .094[a]	− 1.069[a]	− .919[a]
Asymp.Sig. (2-tailed)	.915	.152	.504	.975	.925	.285	.358

TX1, TY1, TZ1: the translation of X, Y, Z-axis for the first registration; TX2, TY2, TZ2: the translation of X, Y, Z-axis for the second registration; RX1, RY1, RZ1: the rotation axis of X, Y, Z-axis for the first registration; RX2, RY2, RZ2: the rotation axis of X, Y, Z-axis for the second registration; R1, R2: the rotation degree for the first and second registration

[a]Based on negative ranks

[b]Based on positive ranks

Table 2 Intra-observer agreement for each of the four image sets (ICC [95% CI])

Observer	No fusion	Fusion 2D	Fusion 3D	Fusion 2D and 3D
Observer 1	0.37 (− 0.01 to 0.67)	0.75 (0.48–0.87)	0.86 (0.69–0.94)	0.80 (0.52–0.92)
Observer 2	0.50 (0.12–0.76)	0.81 (0.57–0.92)	0.76 (0.52–0.89)	0.76 (0.49–0.90)
Observer 3	0.63 (0.28–0.83)	0.70 (0.42–0.86)	0.89 (0.76–0.95)	0.86 (0.69–0.94)

ICC values [20], agreement was rated as "poor" (< 0.50), "moderate" (0.50–0.75), "good" (0.75–0.90), and "excellent" (> 0.90). No fusion: two consecutive CBCT images without fusing; fusion 2D, fused image shown in 2D cross-sectional; fusion 3D: fused image shown in 3D; fusion 2D and 3D: combine fused image shown in 2D cross-sectional and 3D

ROC curves (AUCs) were compared among the four sets using the *Z* test for two independent ROC curves through the MedCalc Statistical Software.

Results

Forty-two TMJs from twenty-one patients were included in this retrospective observational study with a gender predilection of 1:6 (male: 3, female: 18). Their ages ranged from 19 to 70 years, with a mean age of 35.71 ± 17.71 years. The interval between two times of CBCT scanning was 3.4 to 60.6 months, with an average time interval of 12.89 ± 13.01 months. For the registration accuracy evaluation, 26 pairs of TMJs registration were scored as 5 and 16 pairs of TMJs registration were scored as 4. The diagnosis of 9 TMJs (9/42) by the expert panel was inconsistent, and the second evaluation and joint discussion were conducted to reach a consensus. Finally, 24 TMJs were diagnosed as resorption (Figs. 3 and 4), and 18 TMJs were diagnosed as no change (Fig. 2) by the expert panel.

For the repeatability of registration, there were no significant differences in all translational and angular variances between the two times of registration; the *p*-value was more than 0.05 (Table 1).

Intra-observer agreement of the three observers is shown in Table 2. For the set of no fused images, the ICC values for the three observers were 0.37, 0.50, and 0.63, respectively, which indicated a poor to moderate agreement. While for the three sets of fused images, the ICC values from the three observers were moderate to good (0.75, 0.81, and 0.70 for the fused 2D cross-sectional images; 0.86, 0.76, and 0.89 for the fused 3D images; 0.80, 0.76, and 0.86 for the fused 2D cross-sectional images combined with fused 3D images).

Inter-observer agreements of the three observers are shown in Table 3. For the sets of no fused images, the ICC values were moderate to good (0.75 (0.59–0.86)). While for the three fused image sets, the ICC values were good to excellent (0.92 (0.86–0.96) for the fused 2D cross-sectional image sets and fused 3D image sets, 0.91 (0.85–0.95) for the fused 2D cross-sectional image sets combined with 3D image sets.

The values for AUC from each observer for the four image sets are shown in Table 4. The average value of

Table 3 Inter-observer agreement for each of the four image sets (ICC [95% CI])

	ICC	95%CI
No fusion	0.75	0.59 to 0.86
Fusion 2D	0.92	0.86 to 0.96
Fusion 3D	0.92	0.86 to 0.96
Fusion 2D and 3D	0.91	0.85 to 0.95

ICC values [20], agreement was rated as "poor" (< 0.50), "moderate" (0.50–0.75), "good" (0.75–0.90), and "excellent" (> 0.90). No fusion, two consecutive CBCT images without fusing; fusion 2D, fused image shown in 2D cross-sectional; fusion 3D: fused image shown in 3D; fusion 2D and 3D, combine fused image shown in 2D cross-sectional and 3D

Table 4 Area under the receiver operating characteristic curve (AUC) for the four image sets

	Observer1	Obsever2	Obsever3	Mean	SD	Total (the three observers combined, 95% CI)
No fusion	0.79	0.80	0.84	0.81	0.03	0.81 (0.73–0.87)
Fusion 2D	0.92	0.95	0.95	0.94	0.02	0.94 (0.89–0.98)
Fusion 3D	0.90	0.94	0.94	0.93	0.02	0.93 (0.87–0.97)
Fusion 2D and 3D	0.91	0.94	0.95	0.93	0.02	0.94 (0.88–0.97)

No fusion, two consecutive CBCT images without fusing; fusion 2D, fused image shown 2D cross-sectional; fusion 3D, fused image shown in 3D; fusion 2D and 3D, combine fused image shown in 2D cross-sectional and 3D

AUC for the no fused image sets was 0.81, which was smaller than the three fused image sets (0.94, 0.93, 0.93 respectively). Receiver operating characteristic curves (ROCs) from the pooled data of three observers are shown in Fig. 5. The differences between the no fused image sets and the three fused image sets were statistically significant, and there were no statistically significant differences between any two fused image sets (Table 5). The three observers' sensitivity, specificity, PPV, NPV, and accuracy obtained from a pooled data for the four image sets are shown in Table 6.

Discussion

In the present study, the diagnostic accuracy of condylar bone resorption over time was evaluated with the method of image fusion. Compared with the direct observation of condylar bone changes in the CBCT images taken at different time points, the fused CBCT image has higher diagnostic accuracy than that of individual CBCT images when the areas under the ROC curves were evaluated. Further analysis indicated that the AUC values for the three fused image sets were very close and not significantly different. This means

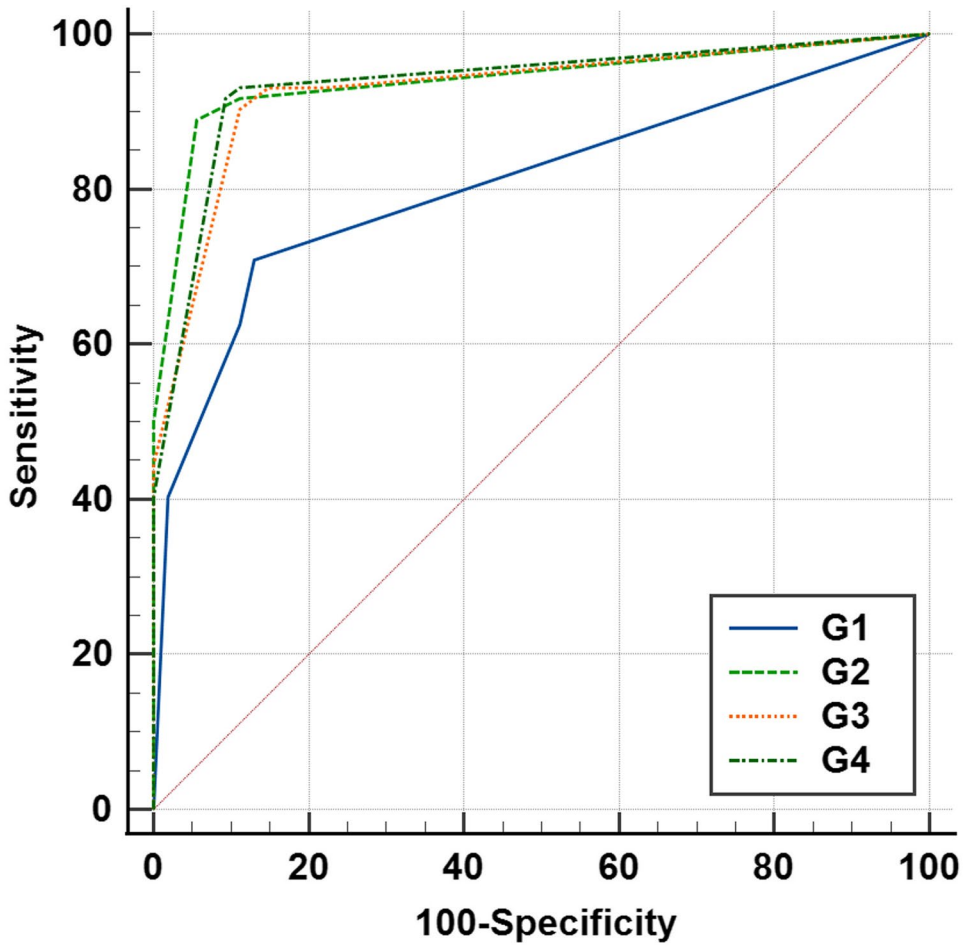

Fig. 5 Receiver operating characteristic curves for the four image sets from pooled data for the resorption of condyle bone. G1, two consecutive CBCT images without fusion; G2, fused 2D cross-sectional images; G3, fused 3D images; G4, combined fused 2D cross-sectional images and fused 3D images

Table 5 *p*-values when comparing AUC of each image set

	Fusion 2D	Fusion 3D	Fusion 2D and 3D
No fusion	0.00*	0.00*	0.00*
Fusion 2D	–	0.60	0.86
Fusion 3D	–	–	0.72

*Significant difference between the no fusion set and others for AUC. No fusion, two consecutive CBCT images without fusing; fusion 2D, fused image show in 2D cross-sectional; fusion 3D, fused image shown in 3D; fusion 2D and 3D, combine fused image shown in 2D cross-sectional and 3D

Table 6 Sensitivity, specificity, PPV, NPV, and accuracy for the four image sets obtained from a pooled data

	Sensitivity	Specificity	PPV	NPV	Accuracy
No fusion	0.708	0.870	0.879	0.691	0.778
Fusion 2D	0.917	0.889	0.917	0.889	0.905
Fusion 3D	0.930	0.852	0.893	0.902	0.897
Fusion 2D and 3D	0.930	0.889	0.918	0.906	0.913

No fusion, two consecutive CBCT images without fusing; fusion 2D, fused image shown in 2D cross-sectional; fusion 3D: fused image shown in 3D; fusion 2D and 3D, combine fused image shown in 2D cross-sectional and 3D

PPV positive predictive value, *NPV* negative predictive value

that the diagnostic accuracy of condylar bone resorption was not further improved with the combined observation of the fused 2D and 3D image sets.

Liu MQ et al. and Koyama J et al. used the direct observation method to evaluate condylar bone changes. However, diagnostic accuracy and reliability were not provided [11, 21]. Ok SM et al. used OnDemand 3D software to superimpose two time points of CBCT images and evaluate the condylar bone changes through 2D cross-sectional CBCT images [13]. Unlike the present study, they did not evaluate bony changes through the fused 2D cross-sectional images but through the separated images at the same angle obtained from the registration process for specific areas. Lee JH et al. and Jiang YY et al. applied the color-coded map to the reconstructed condylar 3D surface that was obtained from the process of segmentation and superimposition of two consecutive CBCT images for qualitative and quantitative evaluation. The results from this study showed that superimposition was an effective tool for the observation of condylar bone remodeling after orthognathic/orthodontic treatment [15, 16].

The intra- and inter-observer consistency indicated by the ICC values was higher for the fused image sets than for the image set without fusing. However, for the three sets of fused images, the intra-observer consistency indicated by the ICC values for the fused 2D&3D image sets was not higher than that of the fused 2D cross-sectional image sets or the fused 3D image sets alone. For observers 1 and 3, the ICC values of the 2D&3D were between the values of the fused 2D sets and the fused 3D sets. And for observer 3, the ICC value of the 2D&3D was lower than that of the fused 2D set and similar to the fused 3D set. Similarly, the inter-observer consistency indicated by the ICC value for the fused 2D&3D image sets (0.91) was slightly lower than that of the fused 2D and 3D image sets (0.92). These results indicated that the combined observation of fused 2D and 3D image sets cannot further improve the intra- and inter-observer consistency.

CBCT is increasingly used as an imaging modality in the assessment of temporomandibular joints due to its high spatial resolution, high detection accuracy in surface osseous changes [6], low radiation dose, and low cost [6, 7, 22]. Studies indicate that CBCT images provide superior reliability and greater accuracy than panoramic radiology [23, 24] and linear tomography [23] in assessing TMJ bone changes. Wang YH et al. reported that in detecting condylar bone defects, the diagnostic accuracy of CBCT was superior to MRI [25]. The result was in line with the study by Schnabl D et al. who reported that osseous alterations such as erosions, osteophytes, and cysts detected by CBCT could not partly be discerned by MRI [26]. Hintze H et al. reported that there were no significant differences in diagnostic accuracy for the detection of bone changes in the condyle between CBCT and conventional tomography [27]. Based on the above evidence, nowadays, CBCT is considered an ideal imaging modality for the detection of condylar bone changes.

By the image registration and fusion method proposed in the present study, two CBCT image sets were fused. The bony changes for cases with minor bone resorption (Fig. 3g–l) or the cases with an irregular and fuzzy bone edge can be intuitively displayed, which may be ignored by observing two separated CBCT images (Fig. 3a–f). This may be helpful to clinicians in the determination of condylar bone changes. For patients with TMJ osteoarthrosis (OA) accompanied by malocclusion and/or facial deformities, only when the condylar bone reaches a stable state and maintains for a certain period, orthodontic treatment and/or orthognathic surgery can be carried out [28, 29]. In such cases, identifying minor condylar bone changes was important. Schilling J et al. also demonstrated that the bone in TMJ condyle is the site of numerous dynamic morphological transformations, which are an integral part of the initiation/progression of OA [30]. Thus, timely and accurate detection of minor condylar bone resorption was important, and the current study has demonstrated the improved efficacy of fused CBCT images on diagnostic accuracy according to Fryback and Thornbury's hierarchical model of efficacy [31]. The efficacy of fused CBCT images on therapeutic thinking and TMJ OA treatment outcome need to be investigated in future studies.

To reduce the influence of background and soft tissue images on the observation, gray values were adjusted to keep them at the same threshold range in the CBCT images taken at two time points before the fusion of 2D cross-sectional and 3D images. The lower limit of the threshold was between 200 and 300, and the upper limit was between 1400 and 1500. For the reconstruction of 3D images, segmentation was the first step. When compared with manual or semi-automatic segmentation [18, 30, 32], which needs to check the segmentation results slice by slice in all three planes (axial, sagittal, coronal), the segmentation based on threshold took only a few to dozen seconds.

Han K et al. reported that both resorption and apposition were observed in condyles with TMJ osteoarthrosis, and resorption/apposition patterns were associated with its sites [18]. However, in the present study, only bone resorption was investigated. This is not limited to the value of the present study since when bone apposition is expected, the fused image is just like the display of bone resorption by changing the order of primary and overlap data.

One limitation of the study is the lack of a gold standard. This problem is common in clinical study when the involved patients have conservative treatment [25, 33]. To solve this problem, the diagnosis from a panel of experts is usually used as a reference standard. In the present study, three specialists' assessment in bone resorption was taken as a reference standard.

Conclusion

It is feasible to visualize the condylar bone resorption by fusing single-mode time series image sets. The consistency and diagnostic accuracy on the detection of condylar bone resorption are improved compared to the direct observation of two consecutive CBCT images. Especially, the fused images can intuitively display condylar bone resorption over time.

Author contribution Feng Ji-ling designed and conducted the experiments, analyzed the results, wrote the main manuscript text, and prepared all the figures and tables. Ma Ruo-han, Du han, Zhao Yan-ping, and Meng Juan-hong conducted the experiments. Li Gang designed and conducted the experiments and made an essential revision to the manuscript. All the authors reviewed the manuscript.

Funding The study was supported by the PKU Baidu Fund (No. 2020BD037) and the National Natural Science Foundation of China (No. 81671034).

Declarations

Competing interests The authors declare no competing interests.

Ethics approval All procedures performed in the study involving human participants were in accordance with the ethical standards of the Institutional Review Board of Peking University School and Hospital of Stomatology and with the 1964 Helsinki declaration and its later amendments or comparable ethical standards. The study was approved by the Institutional Review Board of Peking University School and Hospital of Stomatology (PKUSSIRB-201944056).

Informed consent Written informed consent was not required for this study because all the included patients in the present investigation were collected retrospectively. Exemption of informed consent will not affect the rights and health of included patients. The application for free informed consent has been approved by the Institutional Review Board.

References

1. Wang XD, Kou XX, Mao JJ, Gan YH, Zhou YH (2012) Sustained inflammation induces degeneration of the temporomandibular joint. J Dent Res 91:499–505. https://doi.org/10.1177/0022034512441946
2. Milam SB, Zardeneta G, Schmitz JP (1998) Oxidative stress and degenerative temporomandibular joint disease: a proposed hypothesis. J Oral Maxillofac Surg 56:214–223. https://doi.org/10.1016/s0278-2391(98)90872-2
3. Mao JJ, Rahemtulla F, Scott PG (1998) Proteoglycan expression in the rat temporomandibular joint in response to unilateral bite raise. J Dent Res 77:1520–1528. https://doi.org/10.1177/00220345980770070701
4. Ogura N, Satoh K, Akutsu M, Tobe M, Kuyama K, Kuboyama N, Sakamaki H, Kujiraoka H, Kondoh T (2010) MCP-1 production in temporomandibular joint inflammation. J Dent Res 89:1117–1122. https://doi.org/10.1177/0022034510376041
5. Hashimoto K, Kawashima S, Kameoka S, Akiyama Y, Honjoya T, Ejima K, Sawada K (2007) Comparison of image validity between cone beam computed tomography for dental use and multidetector row helical computed tomography. Dentomaxillofac Radiol 36:465–471. https://doi.org/10.1259/dmfr/22818643
6. Zain-Alabdeen EH, Alsadhan RI (2012) A comparative study of accuracy of detection of surface osseous changes in the temporomandibular joint using multidetector CT and cone beam CT. Dentomaxillofac Radiol 41:185–191. https://doi.org/10.1259/dmfr/24985971
7. Honda K, Larheim TA, Maruhashi K, Matsumoto K, Iwai K (2006) Osseous abnormalities of the mandibular condyle: diagnostic reliability of cone beam computed tomography compared with helical computed tomography based on an autopsy material. Dentomaxillofac Radiol 35:152–157. https://doi.org/10.1259/dmfr/15831361
8. Ma RH, Yin S, Li G (2016) The detection accuracy of cone beam CT for osseous defects of the temporomandibular joint: a systematic review and meta-analysis. Sci Rep 6:34714. https://doi.org/10.1038/srep34714
9. Derwich M, Mitus-Kenig M, Pawlowska E (2020) Interdisciplinary approach to the temporomandibular joint osteoarthritis-review of the literature. Medicina (Kaunas) 56:225. https://doi.org/10.3390/medicina56050225
10. Meng JH, Zhang WL, Liu DG, Zhao YP, Ma XC (2007) [Diagnostic evaluation of the temporomandibular joint osteoarthritis using cone beam computed tomography compared with conventional radiographic technology]. Beijing da xue xue bao. Yi xue ban = Journal of Peking University. Health sciences. 39(1):26–29. https://doi.org/10.3321/j.issn:1671-167X.2007.01.008
11. Koyama J, Nishiyama H, Hayashi T (2007) Follow-up study of condylar bony changes using helical computed tomography in patients with temporomandibular disorder. Dentomaxillofac Radiol 36:472–477. https://doi.org/10.1259/dmfr/28078357
12. Park SB, Yang YM, Kim YI, Cho BH, Jung YH, Hwang DS (2012) Effect of bimaxillary surgery on adaptive condylar head remodeling: metric analysis and image interpretation using cone-beam computed

tomography volume superimposition. J Oral Maxillofac Surg 70:1951–1959. https://doi.org/10.1016/j.joms.2011.08.017
13. Ok SM, Lee J, Kim YI, Lee JY, Kim KB, Jeong SH (2014) Anterior condylar remodeling observed in stabilization splint therapy for temporomandibular joint osteoarthritis. Oral Surg Oral Med Oral Pathol Oral Radiol 118:363–370. https://doi.org/10.1016/j.oooo.2014.05.022
14. Cevidanes LH, Styner MA, Proffit WR (2006) Image analysis and superimposition of 3-dimensional cone-beam computed tomography models. Am J Orthod Dentofacial Orthop 129:611–618. https://doi.org/10.1016/j.ajodo.2005.12.008
15. Lee JH, Lee WJ, Shin JM, Huh KH, Yi WJ, Heo MS, Lee SS, Choi SC (2016) Three-dimensional assessment of condylar surface changes and remodeling after orthognathic surgery. Imaging Sci Dent 46:25–31. https://doi.org/10.5624/isd.2016.46.1.25
16. Jiang YY, Sun L, Wang H, Zhao CY, Zhang WB (2020) Three-dimensional cone beam computed tomography analysis of temporomandibular joint response to the Twin-block functional appliance. Korean J Orthod 50:86–97. https://doi.org/10.4041/kjod.2020.50.2.86
17. Ma RH, Li G, Sun Y, Meng JH, Zhao YP, Zhang H (2019) Application of fused image in detecting abnormalities of temporomandibular joint. Dentomaxillofac Radiol 48:20180129. https://doi.org/10.1259/dmfr.20180129
18. Han K, Kim MC, Kim YJ, Song Y, Tae I, Ryu JJ, Lee DY, Jung SK (2021) A long-term longitudinal study of the osteoarthritic changes to the temporomandibular joint evaluated using a novel three-dimensional superimposition method. Sci Rep 11:9389. https://doi.org/10.1038/s41598-021-88940-y
19. Schiffman E, Ohrbach R, Truelove E, Look J, Anderson G, Goulet JP, List T, *et al*. (2014) Diagnostic criteria for temporomandibular disorders (DC/TMD) for clinical and research applications: recommendations of the International RDC/TMD Consortium Network* and Orofacial Pain Special Interest Group†. J Oral Facial Pain Headache. 28:6–27. https://doi.org/10.11607/jop.1151
20. Koo TK, Li MY (2016) A guideline of selecting and reporting intraclass correlation coefficients for reliability research. J Chiropr Med 15:155–163. https://doi.org/10.1016/j.jcm.2016.02.012
21. Liu MQ, Chen HM, Yap AU, Fu KY (2012) Condylar remodeling accompanying splint therapy: a cone-beam computerized tomography study of patients with temporomandibular joint disk displacement. Oral Surg Oral Med Oral Pathol Oral Radiol 114:259–265. https://doi.org/10.1016/j.oooo.2012.03.004
22. Hashimoto K, Arai Y, Iwai K, Araki M, Kawashima S, Terakado M (2003) A comparison of a new limited cone beam computed tomography machine for dental use with a multidetector row helical CT machine. Oral Surg Oral Med Oral Pathol Oral Radiol Endod 95:371–377. https://doi.org/10.1067/moe.2003.120
23. Honey OB, Scarfe WC, Hilgers MJ, Klueber K, Silveira AM, Haskell BS, Farman AG (2007) Accuracy of cone-beam computed tomography imaging of the temporomandibular joint: comparisons with panoramic radiology and linear tomography. Am J Orthod Dentofacial Orthop 132:429–438. https://doi.org/10.1016/j.ajodo.2005.10.032
24. Oliveira SR, Oliveira RDS, Rodrigues ED, Junqueira JLC, Panzarella FK (2020) Accuracy of panoramic radiography for degenerative changes of the temporomandibular joint. J Int Soc Prev Community Dent 10:96–100. https://doi.org/10.4103/jispcd.JISPCD_411_19
25. Wang YH, Ma RH, Li JJ, Mu CC, Zhao YP, Meng JH, Li G (2022) Diagnostic efficacy of CBCT, MRI and CBCT-MRI fused images in determining anterior disc displacement and bone changes of temporomandibular joint. Dentomaxillofac Radiol:20210286. https://doi.org/10.1259/dmfr.20210286
26. Schnabl D, Rottler AK, Schupp W, Boisserée W, Grunert I (2018) CBCT and MRT imaging in patients clinically diagnosed with temporomandibular joint arthralgia. Heliyon 4:e00641. https://doi.org/10.1016/j.heliyon.2018.e00641
27. Hintze H, Wiese M, Wenzel A (2007) Cone beam CT and conventional tomography for the detection of morphological temporomandibular joint changes. Dentomaxillofac Radiol 36:192–197. https://doi.org/10.1259/dmfr/25523853
28. Lei J, Qin S, Fu KY (2017) Preliminary study of the stability of condylar bony changes of the severe temporomandibular joint osteoarthrosis using cone beam computed tomography 24:212–216. https://doi.org/10.3760/j.issn.1674-5760.2017.04.008
29. Posnick JC, Fantuzzo JJ (2007) Idiopathic condylar resorption: current clinical perspectives. J Oral Maxillofac Surg 65:1617–1623. https://doi.org/10.1016/j.joms.2007.03.026
30. Schilling J, Gomes LC, Benavides E, Nguyen T, Paniagua B, Styner M, Boen V, Gonçalves JR, Cevidanes LH (2014) Regional 3D superimposition to assess temporomandibular joint condylar morphology. Dentomaxillofac Radiol 43:20130273. https://doi.org/10.1259/dmfr.20130273
31. Fryback DG, Thornbury JR (1991) The efficacy of diagnostic imaging. Medical decision making : an international journal of the Society for Medical Decision Making 11:88–94. https://doi.org/10.1177/0272989x9101100203
32. Van Luijn R, Baan F, Shaheen E, Bergé S, Politis C, Maal T, Xi T (2021) Three-dimensional analysis of condylar remodeling and skeletal relapse following LeFort-I osteotomy: a one-year follow-up bicenter study. J Craniomaxillofac Surg. https://doi.org/10.1016/j.jcms.2021.09.021
33. Wang YH, Li G, Ma RH, Zhao YP, Zhang H, Meng JH, Mu CC, Sun CK, Ma XC (2021) Diagnostic efficacy of CBCT, MRI, and CBCT-MRI fused images in distinguishing articular disc calcification from loose body of temporomandibular joint. Clin Oral Investig 25:1907–1914. https://doi.org/10.1007/s00784-020-03497-w

Authors and Affiliations

Ji-ling Feng[1] · Ruo-han Ma[1] · Han Du[1,2,3] · Yan-ping Zhao[1,4] · Juan-hong Meng[4] · Gang Li[1]

Ji-ling Feng
jilingfeng@bjmu.edu.cn

Ruo-han Ma
525943920@qq.com

Han Du
duhan0612@163.com

Yan-ping Zhao
Kqzhao@bjmu.edu.cn

Juan-hong Meng
jhmeng@263.net

[1] Department of Oral and Maxillofacial Radiology, Beijing Key Laboratory of Digital Stomatology, Research Center of Engineering and Technology for Computerized Dentistry Ministry of Health & NMPA Key Laboratory for Dental Materials, Peking University School and Hospital of Stomatology, National Center of Stomatology, National Clinical Research Center for Oral Diseases, National Engineering Laboratory for Digital and Material Technology of Stomatology, No.22 Zhongguancun South Avenue, Haidian District, Beijing 100081, People's Republic of China

[2] Shanghai Stomatological Hospital & School of Stomatology, Fudan University, Shanghai, China

[3] Shanghai Key Laboratory of Craniomaxillofacial Development and Diseases, Fudan University, Shanghai, China

[4] Center for Temporomandibular Disorders and Orofacial Pain, Peking University School and Hospital of Stomatology, Beijing, China